THE UNIVERSITY of EDINBURGH

Edinburgh Research Explorer

Effect of ambient pressure on Leidenfrost temperature

OPEN ACCESS

Effect of ambient pressure on Leidenfrost temperature

Daniel Orejon,[1,2,3,*] Khellil Sefiane,[1,3] and Yasuyuki Takata[1,2]

[1]*International Institute for Carbon-Neutral Energy Research (WPI-I2CNER), Kyushu University, 744 Motooka, Nishi-ku, Fukuoka 819-0395, Japan*

[2]*Department of Mechanical Engineering, Thermofluid Physics Laboratory, Kyushu University, 744 Motooka, Nishi-ku, Fukuoka 819-0395, Japan*

[3]*School of Engineering, The University of Edinburgh King's Buildings, Mayfield Road, Edinburgh EH9 3JL, United Kingdom*

The accurate prediction and control of the interaction of liquids with hot surfaces is paramount in numerous areas, including cooling applications. We present results illustrating the effect of ambient pressure on the temperature required for a droplet to levitate over a hot surface, i.e., the Leidenfrost temperature. In the present study the dependence of wetting and levitating temperatures on ambient pressure in a range of subatmospheric pressures is reported. Experimental data indicate that the Leidenfrost temperature decreases with decreasing pressure at subatmospheric pressures. A physical approach for the dependence of Leidenfrost temperature on ambient pressure, based on an analogy with saturation pressure dependence, is proposed. Furthermore, previous literature data for pressures above atmospheric are also included in the analysis to support and validate the proposed approach. In addition, the effect of substrate material, substrate roughness, and type of fluid on the Leidenfrost temperature is discussed.

For centuries scientists and engineers have devoted sustained efforts to further our understanding of the ubiquitous interactions between solid surfaces and liquids [1]. Hydrophobicity and roughness of the substrate, the nature of the liquid, or the substrate temperature are some of the factors reported to strongly influence the interaction between solids and liquids. Particularly, when increasing the temperature of the substrate in contact with a liquid, a layer of vapor sandwiched between the liquid and the solid is formed. In this region, the liquid is prevented from physically contacting the surface. For the case of levitating droplets this phenomenon is known as the Leidenfrost effect [1]. This can have undesirable effects in cooling due to the insulating features of the vapor phase. The dramatic reduction in cooling efficiency can lead to mechanical failure or even to burnout of the heating surface. This is of paramount importance to applications such as the nuclear industry. On the other hand, and for other purposes, the levitation of the liquid can be desirable as the cushion of vapor allows for almost frictionless motion of a droplet over a heated substrate, which is of great importance for liquid manipulation [2,3].

Since the pioneering observations of Leidenfrost [1], the phenomenon has been sparsely investigated, until very recently where a growing interest in the control of the Leidenfrost phenomenon is driven by the ability to fine-tune substrate properties and hence control the phenomenon. Geometry and shape of the substrate, size and height of the pillars, or the layout and distance between these artificial structures are some of the factors studied [3,4].

Liu and Craig studied the effect of hydrophobicity on Leidenfrost temperature for smooth and flat substrates [5]. It was found that lower substrate temperatures were required for the levitation of a droplet on hydrophobic substrates. Bernardin

and Mudawar [6] addressed, experimentally, the effect of substrate finish on Leidenfrost temperature. An increase in levitating temperature was reported when increasing substrate roughness; however no quantitative evaluation was carried out. More recently, Kwon *et al.* [4] exploited the interplay between surface structures (pillars) and the Leidenfrost phenomenon. The authors achieved a shift in Leidenfrost temperature of more than $100\,°C$ on the same substrate material, when modifying the distance between these structures. Another impressive achievement is the more stable vapor layer reported by Vakarelski *et al.* when immersing a heated metal sphere in a liquid [7]. The absence of nucleate boiling on these textured spheres was achieved by a combination of surface heterogeneities and chemical modification of the substrate.

In addition to these recent studies, other factors such as ambient pressure have attracted the attention of researchers much earlier [8,9]. Emmerson analyzed, experimentally, the effect of high pressure on the temperature required for a water droplet to levitate. The author predicted that Leidenfrost temperature would vary with saturation temperature and found that higher substrate temperatures were required when increasing the ambient pressure although no empirical correlation was proposed [8]. Also Testa and Nicotra observed a decrease in substrate temperature when reducing the pressure of the system below atmospheric [9].

Besides experimental studies on the Leidenfrost phenomenon it is noted that limited theoretical models are available to predict Leidenfrost dependence on ambient pressure. Baumeister and Simon proposed an empirical correlation between the Leidenfrost temperature, thermal conductivity, density, and specific heat of the substrate. However, the effect of pressure or substrate roughness was not taken into account [10]. A few years later, Lienhard proposed a simpler correlation, for system pressures above atmospheric (superatmospheric). The correlation proposed by Lienhard is a function of the critical temperature and saturation temperature
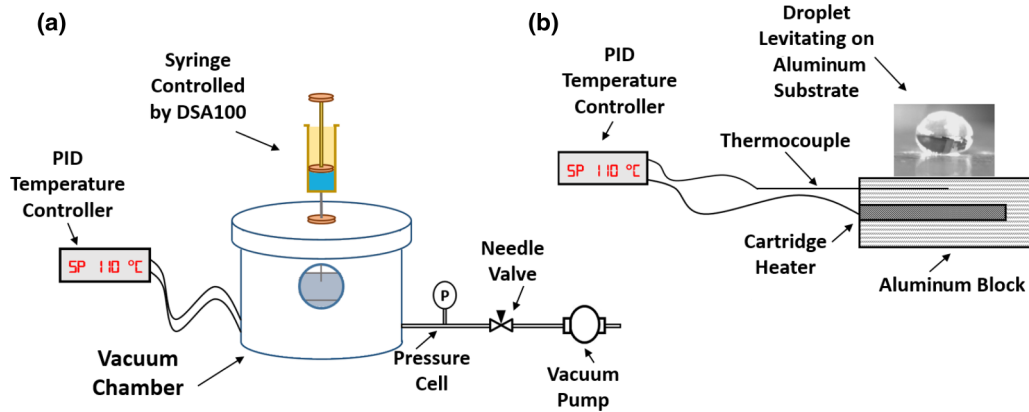
FIG. 1. (Color online) (a) Sketch of the experimental apparatus used in this study and (b) sketch of the heating substrate placed inside the chamber.

[11]. However, this correlation does not indicate any change in Leidenfrost temperature when substituting saturation temperature at subatmospheric pressures.

Despite the effort of researchers over the last decades, studies and correlations addressing the effect of pressure on the Leidenfrost phenomenon remain rather scarce. The very few existing investigations are only suitable for high pressures or for specific substrate materials. Surface finishes such as hydrophobicity and patterned structures are not taken into account as these effects were only revealed recently [4,7]. Lowering the Leidenfrost temperature is proving attractive in the light of recent developments on the use of this phenomenon for liquids and solids manipulation [2,3,12]. Indeed, being able to induce Leidenfrost levitation at lower temperature can make the exploitation of the phenomenon more practical as higher temperatures can be an issue.

A stainless steel low pressure environmental chamber using borosilicate windows and a top lid was used. Additional connections were attached to the chamber, which includes a vacuum pump, pressure cell (± 1 mm Hg), and needle valve to allow for the precise control of the pressure inside the chamber [Fig. 1(a)].

A block of polished aluminum was machined to embed a cartridge heater of 10 kW (maximum power) and a thermocouple inserted a few millimeters beneath the test surface. Both thermocouple and cartridge heater were connected to a proportional-integral-derivative (PID) temperature controller outside the chamber [Fig. 1(b)]. The stainless steel chamber was mounted within the sample stage of a DSA100 (drop shape analyzer, Hamburg, Germany) from Krüss. DSA100 is equipped with an accurate dosing system, back light, and charge-coupled device (CCD) camera for the acquisition of images. DSA1 v1.9 software allowed for the dosing, deposition, and acquisition of images.

First, the planned pressure was achieved using a needle valve connecting the chamber and the vacuum pump. Second, the temperature of the substrate was controlled using an external PID controller. Finally, droplets of approximately 15 μl (droplet radius $\sim$1.5 mm) were produced at the tip of a 0.71$-$mm diameter needle and gently deposited on the aluminum block. The needle tip was lowered at 1 mm/s, and the experiments were recorded at 25 fps.

To rule out any inertial effects during droplet deposition, the Weber number (We $= \rho_f v^2 d / \gamma_{lg}$ where ρ_f is the density of the fluid, v the impact velocity, d the droplet diameter, and γ_{lg} the liquid-gas surface tension) was estimated. It was concluded that inertial effects can be neglected for droplet deposition below 0.1 m/s (this is approximately two orders of magnitude greater than values calculated in the present experiments).

The behavior of a water droplet when deposited on a heated aluminum surface at various ambient pressures is presented. Figure 2 includes a representative depiction of droplet *typical* behavior, employing single snapshots, of the experiments carried out at the same substrate temperature ($T = 105\,°C$) and at different subatmospheric pressures.

From Fig. 2, it is clear that varying ambient (subatmospheric) pressure resulted in noticeably different physical interactions between the droplet and substrate. For a given temperature, three main distinctive regimes can be identified. At "high" pressures, i.e., atmospheric, the observable contact angle at the triple contact line (TCL) characteristic of wetting situations is clear, henceforth referred to as the wetting regime [Fig. 2(a)]. When decreasing the pressure of the system, a transition region or transition regime is observed for 450 and for 300 mm Hg. Violent boiling, droplet disintegration, or droplet breakup takes place within this regime [Figure 2(b)]. When decreasing the pressure of the system further, the droplet adopts a completely spherical shape and rolls over the surface, i.e., Leidenfrost effect, here referred to as the levitating regime. The latter is observed at both 150 and 40 mm Hg [Fig. 2(c)].

The three distinctive regimes presented in Fig. 2 can be clearly identified for the different subatmospheric pressures tested as included in Fig. 3.

In Fig. 3, the wetting Limit, T_W, curve divides the wetting regime from the transition regime and it is found to decrease when reducing the pressure of the system. Likewise the levitating limit or Leidenfrost temperature, T_L, curve can be drawn in between the transition and levitating regimes. T_L also decreases when decreasing pressure. It is worth mentioning the qualitative similarity between T_L and T_W trends presented here when compared with the liquid-vapor saturation curve.

The dependence of T_L on system pressure is consistent with the findings of Emmerson as well as Testa and Nicotra where lower T_L were reported when decreasing system pressure
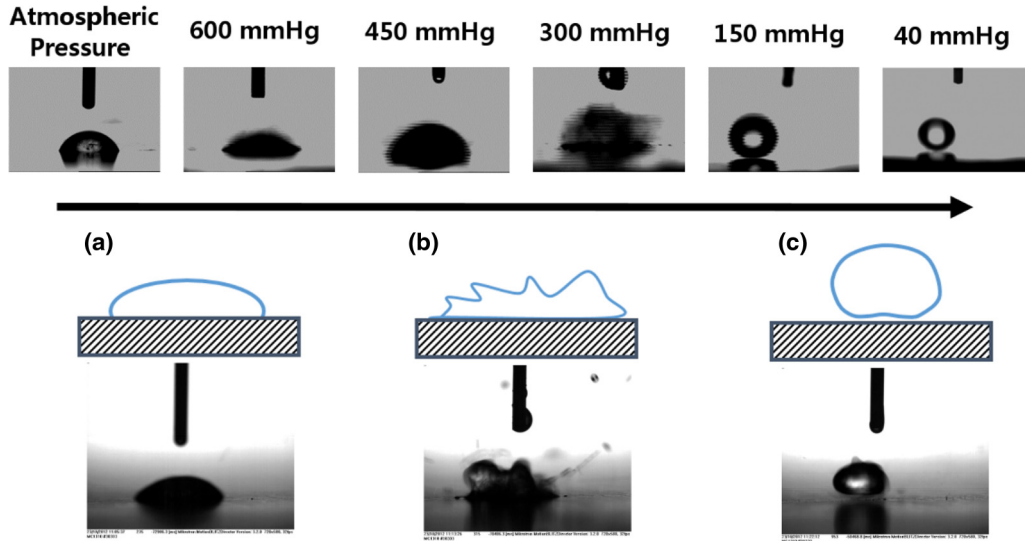
FIG. 2. (Color online) (Top) DSA100 snapshots of a droplet deposited on a heated substrate ($T = 105\,°C$), at different pressures: atmospheric, 600, 450, 300, 150, and 40 mm Hg. (Bottom) Sketch and high speed camera snapshots for the distinctive behaviors: (a) wetting regime, (b) transition regime, and (c) levitating regime.

[8,9], albeit at above-ambient pressures. It is noteworthy that the qualitative correlation between T_W or/and T_L and the liquid-vapor saturation curve was not noted previously; this will be addressed next.

Despite the great importance of fully understanding nucleate boiling, transition boiling, and film boiling as well as other cases involving the Leidenfrost phenomenon for the effective design of heat transfer applications, there is little about it in the literature and only very general empiric correlations to predict T_L. Spiegler *et al.* suggested a correlation to estimate this temperature based on the van der Waals equation [13]. However, this relationship was solely a function of the critical temperature of the fluid and it did not account for any substrate

property. In order to account for the wetting properties of the liquid and the thermal properties of the substrate, and based on the model of Spiegler *et al.*, Baumeister and Simon later on proposed an empirical correlation in which T_L was a function of thermal conductivity, heat capacity, atomic weight, density, surface tension, and temperature of the solid, and the critical temperature and surface tension of the liquid [10]. However, in this correlation, the effect of ambient pressure was not taken into account. The effect of high pressure was thereafter addressed by Lienhard based on a Maxwell–van der Waals equation of state, Eq. (1) [11]:

$$T_L = T_c \left[0.905 + 0.095 \left(\frac{T_{\text{sat}}}{T_c} \right)^8 \right]. \tag{1}$$

Equation (1) is simply a function of the critical temperature, T_c, and the saturation temperature, T_{sat}, of the fluid at a given pressure. This equation agreed quite well with Lienhard experimental data and also provided an account for the observed increase in T_L when increasing the pressure of the system reported by Emmerson [8]. However, as the correlation proposed by Spiegler *et al.*, Eq. (1) also fails to include any substrate property and deviates from experimental data when substituting the relationship T_{sat}/T_c by P_{sat}/P_c at any given pressure.

In this study we propose a different physical approach to predict T_L at subatmospheric pressure. This approach is based on the liquid-vapor saturation curve using a simplified Clausius-Clapeyron equation derived from first principles. After integrating the Clausius-Clapeyron equation, rearranging the terms, and using fitting parameters instead of physical properties, a simplified version of the equation can be obtained, Eq. (2):

$$\frac{1}{T_{\text{sat}}} = A' - B' \ln[P_{\text{sat}}], \tag{2}$$

where A' and B' are fitting constants. Following the same form of dependence of T_{sat} on P_{sat} from Eq. (2), T_L dependence on
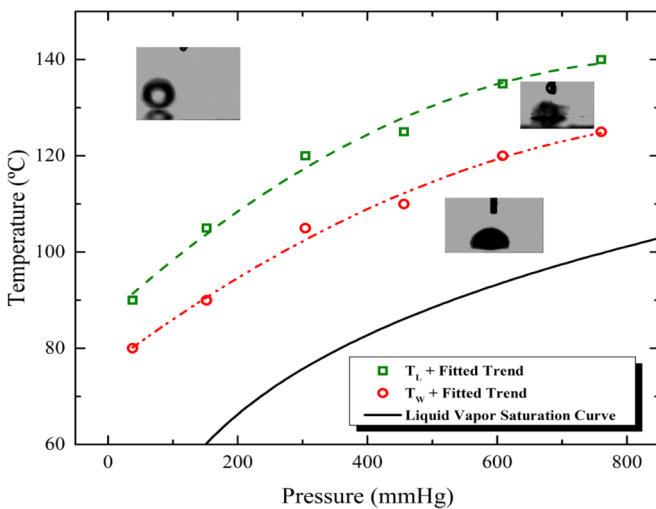

FIG. 3. (Color online) Experimental results and fitted trends for (squares) Leidenfrost temperature, T_L (deg C), and (circles) wetting temperature, T_W (deg C), versus pressure (mm Hg). Liquid-vapor saturation curve from National Institute of Standards and Technology (NIST); solid line is included for comparison.
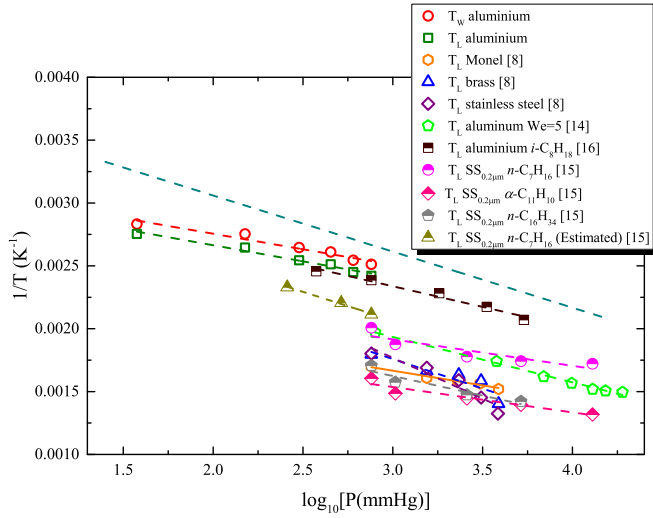
FIG. 4. (Color online) Experimental results of T_L rearranged as $1/T_L$ (K^{-1}) versus $\log_{10}[P(mm\,Hg)]$ for water on (open squares) aluminum, (open hexagons) Monel [8], (open triangles) brass [8], (open diamonds) stainless steel (rms = 0.34 μm) [8], and (open pentagons) aluminum [14]. (Top-full squares) iso-octane on aluminum [16] and (top-full circles) n-heptane, (top-full diamonds) α-methylnaphthalene and (top-full pentagons) n-hexadecane on stainless steel (rms = 0.2 μm) [15]. (Top-full triangles) estimated T_L under pressure for n-heptane on stainless steel (rms = 0.2 μm) [15]. (Open circles) T_W for water on aluminum is also presented. Linear trends as $1/T$ versus $\log_{10}[P]$ and linear trend without symbols for $1/T_{sat}$ versus $\log_{10}[P_{sat}]$ are included to support the discussion. Note that different sets of experimental data exhibit different slopes since these latter depend on the nature and state of the heating substrate as well as the fluid.

ambient pressure, P, is written as

$$\frac{1}{T_L} = A - B\log_{10}[P].\qquad(3)$$

Equation (3) is a correlation for Leidenfrost temperature, T_L, dependence on ambient pressure, P, with two fitting constants A and B, analogous to the simplified Clausius-Clapeyron equation, Eq. (2). In what follows we refer to Eq. (3) as Leidenfrost correlation. The physical argument for using this form will be discussed later on. Since we propose that for droplets gently deposited on a substrate, T_L must be closely correlated to T_{sat} a linear regression to our experimental results is drawn in a form similar to Eq. (3) ($1/T_L$ versus $\log_{10}[P]$). Furthermore, we show that our findings are consistent with Emmerson's experimental results [8] and those of other authors [14–16], at different pressures, as shown in Fig. 4.

Figure 4 shows a satisfactory qualitative agreement in trend between our experimental results for T_L in terms of dependence on ambient pressure. To validate our experimental findings against the proposed correlation, data from the literature [8,14–16] have also been reviewed and included together with our experimental results in Fig. 4. For the different materials studied (aluminum, brass, Monel, and stainless steel), the agreement between the linear regressions $1/T_L$ versus $\log_{10}[P]$ proposed is acceptable. The case of iso-octane included in the work of Stanglmaier *et al.* and different

organic fluids studied by Temple-Pediani, reinforce our idea of relating levitating temperature with saturation temperature dependence on pressure, for sub- and above-ambient pressures.

When comparing the levitating temperature for water at atmospheric pressure, a substantial difference between our experimental results and those of Emmerson is noticed. As mentioned previously, Kwon *et al.* reported a shift in T_L of more than 100 °C when modifying the micro- and nano-features of the substrate [4]. Structured substrates with the same micropost geometry were studied and higher T_L were reported when increasing the spacing between microposts. Spacing the pillars decreases "locally" the area of substrate adjacent to the droplet and therefore the amount of heat flux beneath the droplet. To compensate for those losses and in order for the substrate to supply the necessary heat flux for the droplet to levitate, greater T_L is essential. The necessary heat for Leidenfrost is the amount of energy required to generate enough vapor via evaporation to counter the droplet weight. Furthermore, inhomogeneities on the surface topography might modify the natural flow of vapor underneath the droplet, creating a nonuniform cushion of vapor, i.e., unstable levitation. Bernardin and Mudawar also reported similar differences in the T_L, ~ 80 °C, between polished aluminum and particle blasted aluminum [6]. In the case of Emmerson, the substrates used were found to be rough ($R_{rms\_Brass} = 0.33\ \mu$m, $R_{rms\_Monel} = 0.31\ \mu$m, and $R_{rms\_Stainless\ Steel} = 0.34\ \mu$m [8]) when compared to polished aluminum used in our experiments. This underlines the importance of accounting for substrate topography when identifying the variables directly affecting the levitating behavior.

Next, we address the effect of substrate material on levitating temperature. As Baumeister and Simon reported previously, T_L is a function of thermal conductivity, density, and specific heat of the substrate. Thus, for different materials, different T_L versus pressure are expected, as opposed to the Lienhard interpretation. Table I includes empirical correlations and Leidenfrost temperature at ambient pressure, T_L^*, for the different surfaces present in Fig. 4. It has to be mentioned that the T_L^* reported for iso-octane on aluminum was obtained under droplet impingement conditions whereas the rest are for droplets gently deposited on the substrate.

From Table I, a clear dependence of y intercept point, A, and slope, B, with substrate material is reported. Then the fitting constants A and B are a function of surface properties such as thermal conductivity, density, heat capacity, hydrophobicity, and roughness. Then Eq. (3) might be rewritten as

$$\frac{1}{T_L} = A(\text{surface properties})$$
$$- B(\text{surface properties})\log_{10}[P].\qquad(4)$$

The effect of substrate properties will be discussed next. When comparing the same liquid, i.e., pure water, both A and B empirical values decrease when increasing the reported T_L. Baumeister *et al.* also reported that for high T_L, the heat transfer from the substrate to the droplet was far from isothermal [17]. To discuss the different properties of substrates they proposed the coefficient β, as $\beta = 1/kC\rho$, where k, C, and ρ are the thermal conductivity, heat capacity, and density of the solid, respectively. β is the inverse square

TABLE I. $1/T$ (K^{-1}) versus $\log_{10}[P(\text{mm Hg})]$ Leidenfrost correlation analogous to a simplified Clausius-Clapeyron equation and T_L^* (K) at atmospheric pressure for the different materials.

Surface	Leidenfrost correlation	T_L^*(K)
T_{sat}	$1/T = 0.00395 - 0.000443\log_{10}[P]$	
T_W Aluminum	$1/T_W = 0.00325 - 0.000248\log_{10}[P]$	
T_L Aluminum	$1/T_L = 0.00318 - 0.000256\log_{10}[P]$	413 K
T_L SS$_{0.34\,\mu m}$	$1/T_L = 0.00372 - 0.00065\log_{10}[P]$	555 K [8]
T_L Brass	$1/T_L = 0.00317 - 0.00047\log_{10}[P]$	557 K [8]
T_L Monel	$1/T_L = 0.00237 - 0.000233\log_{10}[P]$	589 K [8]
T_L Aluminum	$1/T_L = 0.00302 - 0.000361\log_{10}[P]$	413 K [14]
$T_L\,i-C_8H_{18}$ on Aluminum	$1/T_L = 0.00332 - 0.000329\log_{10}[P]$	463 K [16]
$T_L\,n-C_7H_{16}$ on SS$_{0.2\,\mu m}$	$1/T_L = 0.00255 - 0.00021\log_{10}[P]$	498 K [15]
$T_L\,\alpha-C_{11}H_{10}$ on SS$_{0.2\,\mu m}$	$1/T_L = 0.00214 - 0.000201\log_{10}[P]$	623 K [15]
$T_L\,n-C_{16}H_{34}$ on SS$_{0.2\,\mu m}$	$1/T_L = 0.00256 - 0.000312\log_{10}[P]$	589 K [15]
$T_L\,n-C_7H_{16}$ on SS$_{0.2\,\mu m}$ (estimated)	$1/T_L = 0.00343 - 0.000455\log_{10}[P]$	473 K [15]

of the thermal effusivity, which accounts for how easy it is for a material to exchange thermal energy with the surroundings. Besides the coefficient β proposed by Baumeister *et al.* to account for the thermal properties of the substrate and in order to describe the isothermal condition of the substrate, we believe it is more relevant to consider thermal diffusivity, α, written as $\alpha = k/\rho C$ [18]. Thermal diffusivity is defined as the ratio of the ability to conduct thermal energy to the capacity to store it. Then if a droplet is deposited on a high thermal diffusivity, α, substrate, the surface of this latter will regain its initial temperature quicker than on lower thermal diffusivity substrates, i.e., insulating ones. Hence a higher thermal diffusivity substrate is expected to be more isothermal. Figure 5 is a comparison of the reported slope of the T_L correlation, B (extracted from Table I), and the thermal diffusivities of the different substrates studied. For this comparison to make sense, the fluid has to be the same. Hence, we selected data for water on three substrates with different thermal diffusivities.
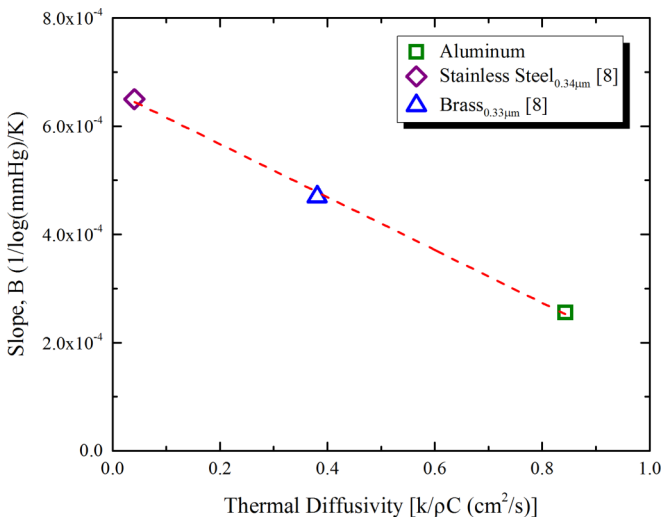

FIG. 5. (Color online) Slope B for water versus thermal diffusivity of (square) aluminum, (diamond) stainless steel, and (triangle) brass.

Figure 5 shows a decrease in the reported value of B when increasing the thermal diffusivity of the substrate. This means that on isothermal substrates, high α, the change in T_L with system pressure is expected to be less severe than on nonisothermal ones. We exclude the case of Monel from our analysis in Fig. 5, since the type of the specific Monel alloy used in Emmerson's experiments was not precisely specified in terms of thermal properties, according to the authors [8].

Adopting the approach presented in Eq. (4), we can relate directly our variables A and B with surface properties; $A, B = f(1/\alpha)$. Then, a greater slope and higher T_L will be expected for nonisothermal substrates. Moreover, and as mentioned above, we certainly must account for the effect of substrate roughness, where greater R_{rms} requires higher T_L for the droplet to levitate; therefore $A, B = f(1/\alpha, R_{\text{rms}})$.

When comparing water and iso-octane on smooth aluminum, T_L is quite similar for pressures ranging from 0.5 to 1 atm, as shown in Fig. 4. The slight difference in the value of the slope is presumably due to the difference in fluid volatility. To support this idea further, we now compare the different alkanes, i.e., n-heptane and n-hexadecane, studied by Temple-Pediani on stainless steel. Lower T_L is found for the more volatile of the alkanes, e.g., n-heptane. Furthermore, we include in the analysis the work of Gottfried *et al.*, where a decrease in T_L^* for more volatile fluids was observed when comparing different alcohols and water [19]. Then we conclude that A and B must also depend on the volatility of the fluid; $A, B = f(1/\alpha, R_{\text{rms}}, 1/P_{\text{sat}})$.

We must stress the fact that all three parameters α, R_{rms}, and P_{sat} contribute equally to T_L^* and therefore to T_L when modifying the pressure of the system. This is demonstrated by the wide range of data (including ours) presented in Fig. 4 and Table I.

The physical argument as to why the saturation temperature dependence on pressure should necessarily be relevant to explain the dependence of T_L on pressure is as follows:

In order for a droplet of a given mass to levitate, this latter has to generate enough vapor at its base to provide lift in order to compensate for the weight. The vapor providing lift is generated by evaporation. It is commonly known that evaporation rate is directly related to saturation temperature of the gas-liquid interface. For instance, in Hertz-Knudsen theory

based on the classical kinetic theory of gases, the evaporation rate is directly related to pressure and temperature at the interface [20,21]. This implies that T_L must account for the dependence of saturation temperature on pressure.

Concerning the physical mechanisms by which other parameters such as roughness, hydrophobicity, and thermal properties of the substrate affect T_L, this is still a debatable question among researchers in this field.

To conclude, in this study the dependence of levitating temperature (Leidenfrost) on ambient pressure is reported. It is shown that the T_L decreases with decreasing pressure, both at sub- and above-ambient pressures. In addition, we propose an approach to correlate T_L with pressure, which is valid at both subatmospheric as well as at superatmospheric pressures. It is suggested that the T_L can be correlated with liquid-vapor saturation curves, i.e., Leidenfrost correlation analogous to the simplified Clausius-Clapeyron equation, when increasing or decreasing the pressure of the system. Also a crude qualitative analysis of the variables governing the proposed correlation is discussed. The agreement between the proposed relationship and experimental results is acceptable and offers a direction for the analysis and prediction of droplet levitation phenomena when changing the nature of the substrate (intrinsic properties of the material and roughness) and the fluid, under different system pressures. This opens anotherway for the interpretation of studies dealing with Leidenfrost temperature dependence on ambient pressure.

---

[1] J. G. Leidenfrost, *De Aquae Communis Nonnullis Qualitatibus Tractatus*, 1756; Int. J. Heat Mass Transfer **9**, 1153 (1966) (translated by C. Wares).

[2] G. Lagubeau, M. Le Merrer, C. Clanet, and D. Quéré, Nat. Phys. **7**, 395 (2011).

[3] H. Linke, B. J. Alemán, L. D. Melling, M. J. Taormina, M. J. Francis, C. C. Dow-Hygelund, V. Narayanan, R. P. Taylor, and A. Stout, Phys. Rev. Lett. **96**, 154502 (2006).

[4] H. Kwon, J. C. Bird, and K. K. Varanasi, Appl. Phys. Lett. **103**, 201601 (2013).

[5] G. Liu and V. S. J. Craig, Faraday Discuss. **146**, 141 (2010).

[6] J. D. Bernardin and I. Mudawar, J. Heat Transfer **121**, 894 (1999).

[7] I. U. Vakarelski, N. A. Patankar, J. O. Marston, D. Y. C. Chan, and S. T. Thoroddsen, Nature **489**, 274 (2012).

[8] G. S. Emmerson, Int. J. Heat Mass Transfer **18**, 381 (1975).

[9] P. Testa and L. Nicotra, J. Heat Transfer **108**, 916 (1986).

[10] K. J. Baumeister and F. F. Simon, J. Heat Transfer **95**, 166 (1973).

[11] J. H. Lienhard, Chem. Eng. Sci. **31**, 847 (1976).

[12] T. Baier, G. Dupeux, S. Herbert, S. Hardt, and D. Quéré, Phys. Rev. E **87**, 021001(R) (2013).

[13] P. Spiegler, J. Hopenfeld, M. Silberberg, C. F. Bumpus, Jr., and A. Norman, Int. J. Heat Mass Transfer **6**, 987 (1963).

[14] I. Buchmüller, Ph.D. Dissertation from the Technical University of Darmstadt, 2014.

[15] R. W. Temple-Pediani, Proc. Inst. Mech. Eng. **184**, 677 (1969).

[16] R. H. Stanglmaier, C. E. Roberts, and C. A. Moses, SAE Technical Paper 2002-01-838, 2002.

[17] K. J. Baumeister, R. E. Henry, and F. F. Simon, NASA Technical Report Server NASA Report/Patent Number: NASA-TM-X-52866, E-5828 (1970).

[18] T. L. Bergman, A. S. Lavine, F. P. Incropera, and D. P. Dewitt, *Fundamentals of Heat and Mass Transfer*, 7th ed. (John Wiley and Sons Inc., New York, 2011).

[19] B. S. Gottfried, C. J. Lee, and K. J. Bell, Int. J. Heat Mass Transfer **9**, 1167 (1966).

[20] H. Hertz, Ann. Phys. (Leipzig) **253**, 177 (1882).

[21] M. Knudsen, Ann. Phys. (Leipzig) **352**, 697 (1915).